



Contents lists available at SciVerse ScienceDirect

## Bioorganic &amp; Medicinal Chemistry

journal homepage: [www.elsevier.com/locate/bmc](http://www.elsevier.com/locate/bmc)

## Conformational analysis of two novel cytotoxic C2-substituted pyrrolo[2,3-*f*]quinolines in aqueous media, organic solvents, membrane bilayers and at the putative active site

Nicole Varvarigou<sup>a</sup>, Grigorios Megariotis<sup>b</sup>, Georgios Leonis<sup>b</sup>, Eleni Vrontaki<sup>a</sup>, Antigoni-Margarita Maniati<sup>a</sup>, Marilena Vlachou<sup>c</sup>, Aphrodite Eikospentaki<sup>c</sup>, Rodanthi Kompogennitaki<sup>d</sup>, Manthos G. Papadopoulos<sup>b</sup>, Simona Golic Grdadolnik<sup>e,f</sup>, Dimitri Komiotis<sup>g</sup>, Thomas Mavromoustakos<sup>a,\*</sup>, Andrew Tsotinis<sup>d,\*</sup>

<sup>a</sup> National and Kapodistrian University of Athens, Chemistry Department, Laboratory of Organic Chemistry, Panepistimioupoli-Zografou, 15771 Athens, Greece

<sup>b</sup> National Hellenic Research Foundation, Institute of Biology, Medicinal Chemistry and Biotechnology, Vas. Constantinou 48, 11635 Athens, Greece

<sup>c</sup> National and Kapodistrian University of Athens, Faculty of Pharmacy, Department of Pharmaceutical Technology, Panepistimioupoli-Zografou, 15771 Athens, Greece

<sup>d</sup> National and Kapodistrian University of Athens, Faculty of Pharmacy, Department of Pharmaceutical Chemistry, Panepistimioupoli-Zografou, 15771 Athens, Greece

<sup>e</sup> Laboratory of Biomolecular Structure, National Institute of Chemistry, Hajdrihova 19, SI-1001 Ljubljana, Slovenia

<sup>f</sup> EN-FIST Centre of Excellence, Dunajska 156, SI-1000 Ljubljana, Slovenia

<sup>g</sup> Department of Biochemistry and Biotechnology, Laboratory of Organic Chemistry, University of Thessaly, 41221 Larissa, Greece

## ARTICLE INFO

## Article history:

Received 21 May 2012

Revised 1 September 2012

Accepted 7 September 2012

Available online 15 September 2012

## Keywords:

Cytotoxic agents

Conformational analysis

NMR spectroscopy

Molecular dynamics

Molecular docking

Lipid bilayers

## ABSTRACT

We have performed: (i) conformational analysis of two novel cytotoxic C2-substituted pyrrolo[2,3-*f*]quinolines **5e** and **5g** in deuterated dimethylsulfoxide (DMSO-*d*<sub>6</sub>) utilizing NOE results from NMR spectroscopy; (ii) molecular dynamics (MD) calculations in water, DMSO and dimyristoyl phosphatidylcholine bilayers and (iii) molecular docking and MD calculations on DNA nucleotide sequences. The obtained results for the two similar in structure molecules showed differences in: (i) their conformational properties in silico and in media that reasonably simulate the biological environment; (ii) the way they are incorporated into the lipid bilayers and therefore their diffusion ability and (iii) molecular docking capacity as it is depicted from their different binding scores.

© 2012 Elsevier Ltd. All rights reserved.

## 1. Introduction

DNA cross-linking agents are known for their significant antitumor activity, which has been attributed to their ability to form irreparable base pair adducts at precisely defined genomic locations.<sup>1</sup> Most of the reported cross-linking probes involve three or four aromatic chromophores in their skeleton and are of sufficient size to recognize two or three base pairs. An extension of this limited sequence recognition, which is attained by the use of larger aromatic heterocycles, has been found to drastically enhance cytotoxicity due to the formation of more rigid irreversible interstrand bonds.<sup>2</sup>

\* Corresponding author. Tel.: +30 2107274474; fax: +30 2107274761 (T.M.); tel.: +30 2107274812; fax: +30 2107274811 (A.T.).

E-mail addresses: [tmavrom@chem.uoa.gr](mailto:tmavrom@chem.uoa.gr) (T. Mavromoustakos), [tsotinis@pharm.uoa.gr](mailto:tsotinis@pharm.uoa.gr) (A. Tsotinis).

In the course of our research towards the development of new DNA-complexing agents, we have previously reported the synthesis and cytotoxic profile of a series of C2-substituted pyrrolo[2,3-*f*]quinolones.<sup>3</sup> To further explore the activity of these agents we have recently published the synthesis and biology of the dimeric pyrrolo[2,3-*f*]quinolines **5e** and **5g** (Fig. 1).<sup>4</sup> The overall size of the skeleton of these molecules has been increased, allowing the new probes to span a larger number of base pairs in order to act as cross-linkers.

The promising diverse biological properties of these compounds led us to apply a combination of NMR data analysis and conformational studies in different biomimetic media in an attempt to understand and correlate their biological properties. The results obtained show that although the two molecules possess very similar chemical structures, they are characterized by different conformational properties, different modes of incorporation in membrane bilayers and of docking in the nucleotide sequences.

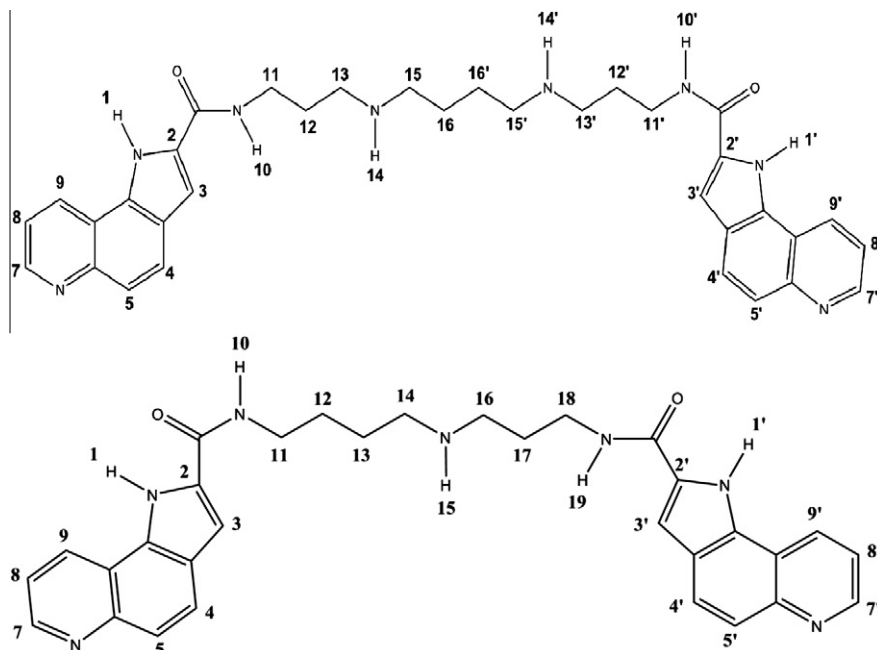


Figure 1. Chemical structures of **5e** (top) and **5g** (bottom).

## 2. Materials and methods

### 2.1. Materials

Compounds **5e** and **5g** were synthesized at Professor's Andrew Tsotinis laboratory by amidating 1*H*-pyrrolo[2,3-*f*]quinolone-2-carboxylic acid<sup>3</sup> with the appropriate  $\alpha,\omega$ -diamine.<sup>4</sup>

### 2.2. Nuclear magnetic resonance experiments

The high-resolution NMR experiments were performed at the National Institute of Chemistry in Slovenia on a Varian DirectDrive 800 MHz spectrometer. Samples for the NMR experiments were dissolved in deuterated DMSO-*d*<sub>6</sub> (1.1 mM solution) and TMS was used as the chemical shift reference.

A two-dimensional (2D) <sup>1</sup>H–<sup>1</sup>H chemical shift correlation spectrum (DQF-COSY) was obtained in order to assign proton resonances of **5e** and **5g**. A 2D <sup>1</sup>H–<sup>1</sup>H Nuclear Overhauser Enhancement (NOESY) was performed to aid the assignment of **5e** and **5g** and to study their conformational properties. Spectra were collected in the phase sensitive mode using the pulse sequences in the Varian library of pulse programs. All data were analyzed using MestReNova Version 6.2.1.

### 2.3. Molecular modeling—molecular dynamics

Initial structures of **5e** and **5g** were generated using a 2D sketcher module of SYBYL 8.0 molecular modeling interface. Next, Gromacs topologies and pdb files, for both **5e** and **5g**, were generated in extended conformations using the JME editor (2D sketcher module) in the DUNDEE PRODRG server (<http://dav-apc1.bioch.dundee.ac.uk/prodrng/>).<sup>5</sup>

#### 2.3.1. Compounds **5e** and **5g** in water and in DMSO

Molecular dynamics (MD) simulations were performed using the MD package GROMACS 4.5.1.<sup>6–8</sup> Each molecule was constructed with the ANTECHAMBER module (using the general AMBER GAFF force field)<sup>9,10</sup> and atomic partial charges were assigned with the AM1-BCC method.<sup>11</sup>

The canonical ensemble (NVT) at 300 K with periodic boundary conditions was used and the temperature was kept constant with the Berendsen thermostat.<sup>12</sup> Electrostatic interactions were calculated using the particle mesh Ewald (PME) method.<sup>13</sup> Cutoff distances for the calculation of Coulomb and van der Waals interactions were 1.4 nm. The cubic elementary box containing **5e** or **5g** and  $\approx$ 4000 water molecules was described by the Simple Point Charge (SPC) model<sup>14</sup>, yielding an average density of 0.996 g/cm<sup>3</sup>. Prior to the dynamics simulation, energy minimization was applied to each system (**5e** or **5g** with solvent water molecules) without constraints, using the Steepest Descent integrator for 1000 steps. Finally, two all atom, unrestrained 40 ns MD simulations were performed at 300 K with a time step of 1 fs. The effect of solvation on the conformations was also examined by changing the solvent from water to a pre-equilibrated DMSO box (containing approximately 1200 DMSO molecules).

Table 1

<sup>1</sup>H NMR chemical shift assignments of **5e** fumarate in DMSO solution (1.1 mM)

Hydrogen	Chemical shift (ppm)	# of hydrogens	Multiplicity (J)
1, 1'	12.97	1	m
	12.74	1	m
3, 3'	7.32	2	s
4, 4'	7.59	2	d ( <i>J</i> = 8.8 Hz)
5, 5'	7.92	2	d ( <i>J</i> = 8.9 Hz)
7, 7'	9.17	1	d ( <i>J</i> = 8.4 Hz)
	9.15	1	d ( <i>J</i> = 8.2 Hz)
8, 8'	7.54	2	m
9, 9'	8.80	2	dd ( <i>J</i> = 10.8, 3.6 Hz)
10, 10'	8.88	2	s
11, 11'	3.39–3.42	4	m
12, 12'	1.87	2	quin
	1.80	2	quin
13, 13'	2.88	3	br
	2.58	1	br
14, 14'	2.54	1	m
	2.52	1	m
15, 15'	2.81	3	br
	2.68	1	br
16, 16'	1.64	2	m
	1.56	2	m
Fumarate	6.50	4	s

**Table 2**  
<sup>1</sup>H NMR chemical shift assignments of **5g** fumarate in DMSO-*d*<sub>6</sub> solution (1.1 mM)

Hydrogen	Chemical shift (ppm)	# of hydrogens	multiplicity (J)
1, 1'	12.77	2	s
3, 3'	7.30	2	s
4, 4'	7.58	4	d (J = 8.8 Hz)
5, 5'	7.91	1	d (J = 8.8 Hz)
	7.90	1	s
7, 7'	9.15	2	dd (J = 4.2, 1.4 Hz)
8, 8'	7.53	2	dd (J = 8.3, 4.2 Hz)
9, 9'	8.79	2	d (J = 8.1 Hz)
10, 19	8.64	2	bs (J = 4.8 Hz)
11, 18	3.38–3.41	4	m
12, 13, 17	1.78	6	quin
14, 16	2.58	1	m
	2.54	1	m
	2.52	2	m
15	2.29	1	s
Fumarate	6.50	4	s

### 2.3.2. Compounds **5e** and **5g** in lipid bilayers

Drug topology files were produced using the PRODGR server as mentioned above. For dimyristoylphosphatidylcholine (DMPC) molecules, the united atom representation was adopted and the topology files were downloaded from the Tieleman web page (<http://people.ucalgary.ca/~tieleman/download.html>)<sup>15,16</sup>, while water molecules were described by the Simple Point Charge (SPC) model. The simulated bilayer system consisted of 128 DMPC molecules in the liquid-crystalline phase and 3655 water molecules. All simulations were performed with the MD package GRO-MACS 4.5.1. Equations of motion were integrated with a time step equal to 2 fs and all bonds were constrained to their equilibrium length with a harmonic force constant of 1000 kJ mol<sup>-1</sup> nm<sup>2</sup>, using

the LINCS algorithm.<sup>17</sup> The temperature was kept constant at 310 K using a Berendsen thermostat with a coupling time constant equal to 0.1 ps, while the Berendsen barostat was employed for the semi-isotropic pressure coupling of the system at 1 bar. The latter means that the Z-direction, which is perpendicular to the two monolayers, is coupled independently from the XY plane but in both cases the coupling time constant was set to 1 ps. Overall, there are two degrees of freedom distributed between Z direction and XY plane, which are set to 1 bar. Long-range electrostatic interactions were treated with the PME method, while Coulomb and Lennard-Jones interactions have been calculated using a 1 nm cutoff. MD simulations of the two bilayer systems were run for 100 ns each.

### 2.3.3. Docking and MD calculations of compounds **5e** and **5g** to nucleotide sequences of DNA

Both structures were subjected to energy minimization using the Steepest Descent, Conjugate Gradient and Powell algorithms. Partial charge contributions were calculated by the Gasteiger–Huckel method and a 0.001 kcal/mol energy gradient convergence criterion using the standard Tripos MM force field of the Sybyl molecular modeling package.<sup>18</sup>

Simulated annealing calculations were conducted in vacuum without restraints, over 100 cycles with heating to 2000 K over 2 ps and subsequent annealing to 0 K over 10 ps, with an exponential function. This method resulted in 100 low-energy conformers that were used for docking calculations.<sup>19,20</sup>

The structures of **5e** and **5g** were docked in the crystal DNA sequence obtained from the Protein Data Bank (code number 1d64)<sup>21</sup> using the 'extra-precision' mode of Glide.<sup>21</sup> This sequence presents a high percentage of pair bases G–C and is complexed with pentamidine, a compound that has similar chemical structure to the molecules under study.<sup>22</sup>

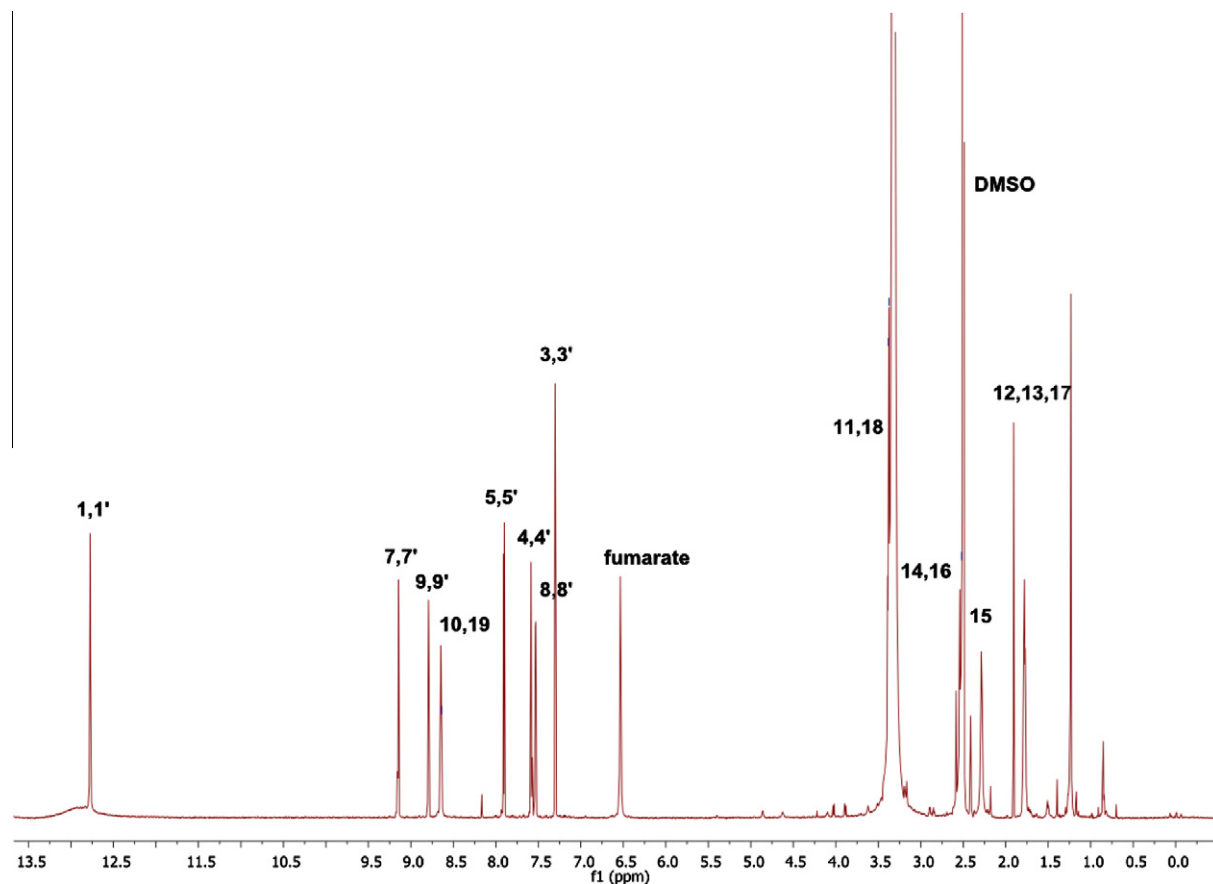


**Figure 2.** <sup>1</sup>H NMR spectrum of **5g** obtained in DMSO-*d*<sub>6</sub> at 25 °C and 800 MHz.

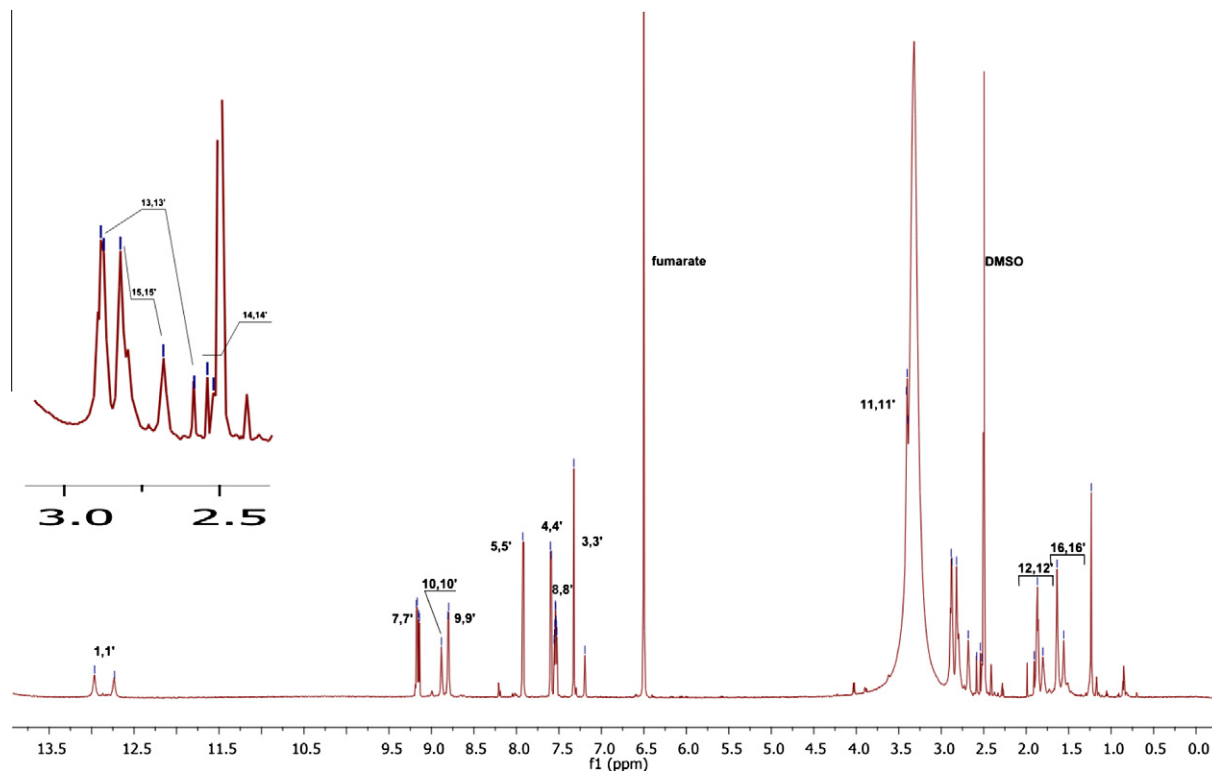


Figure 3.  $^1\text{H}$  NMR spectrum of **5e** obtained in  $\text{DMSO}-d_6$  at  $25^\circ\text{C}$  and 800 MHz.

The DNA sequence for dodecamer 1d64, 5'-d(C-G-C-A-A-T-T-C-G-C-G)-3' was prepared with the Protein Preparation Wizard utility provided by Schrödinger.<sup>23</sup> According to this, bond orders were assigned, crystal water molecules were removed and hydrogen atoms were added. The 3D structure of DNA was further refined using a restraint minimization method for hydrogen atoms only, and constraint was set to  $0.3 \text{ \AA}$  (Force field OPLS 2005).

MD calculations of 1d64-drug complexes were also performed employing the GROMACS package and AMBER-03 all-atom force field.<sup>24</sup> A cubic box with 9014 SPC water molecules was constructed and 22  $\text{Na}^+$  ions were added to neutralize the system.

After manual docking of **5e** or **5g** into 1d64, the compounds were found in the major groove of the double helix. The whole system was initially energy-minimized using the steepest descent method. MD simulations were then performed, initially with position restraints (for the first 10 ns) and subsequently fully unrestrained (for additional 40 ns). The time step was equal to 2 fs with all bonds constrained to their equilibrium length using the LINCS algorithm. Temperature and pressure were kept constant at 310 K and at 1 bar, with time constants of 0.1 and 1 ps for the Berendsen thermostat and barostat, respectively. The long range electrostatic interactions were treated with the PME method, while

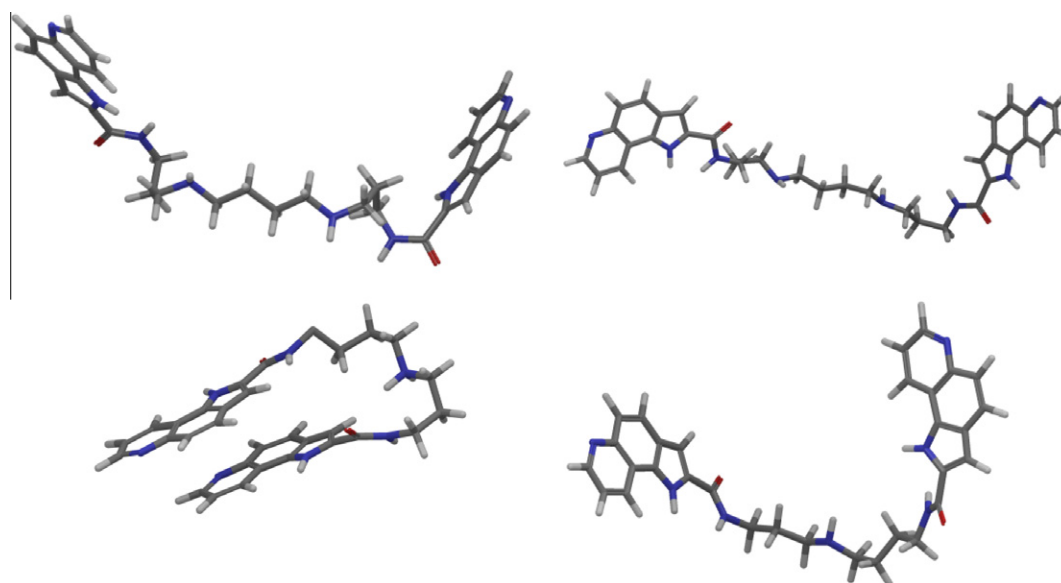
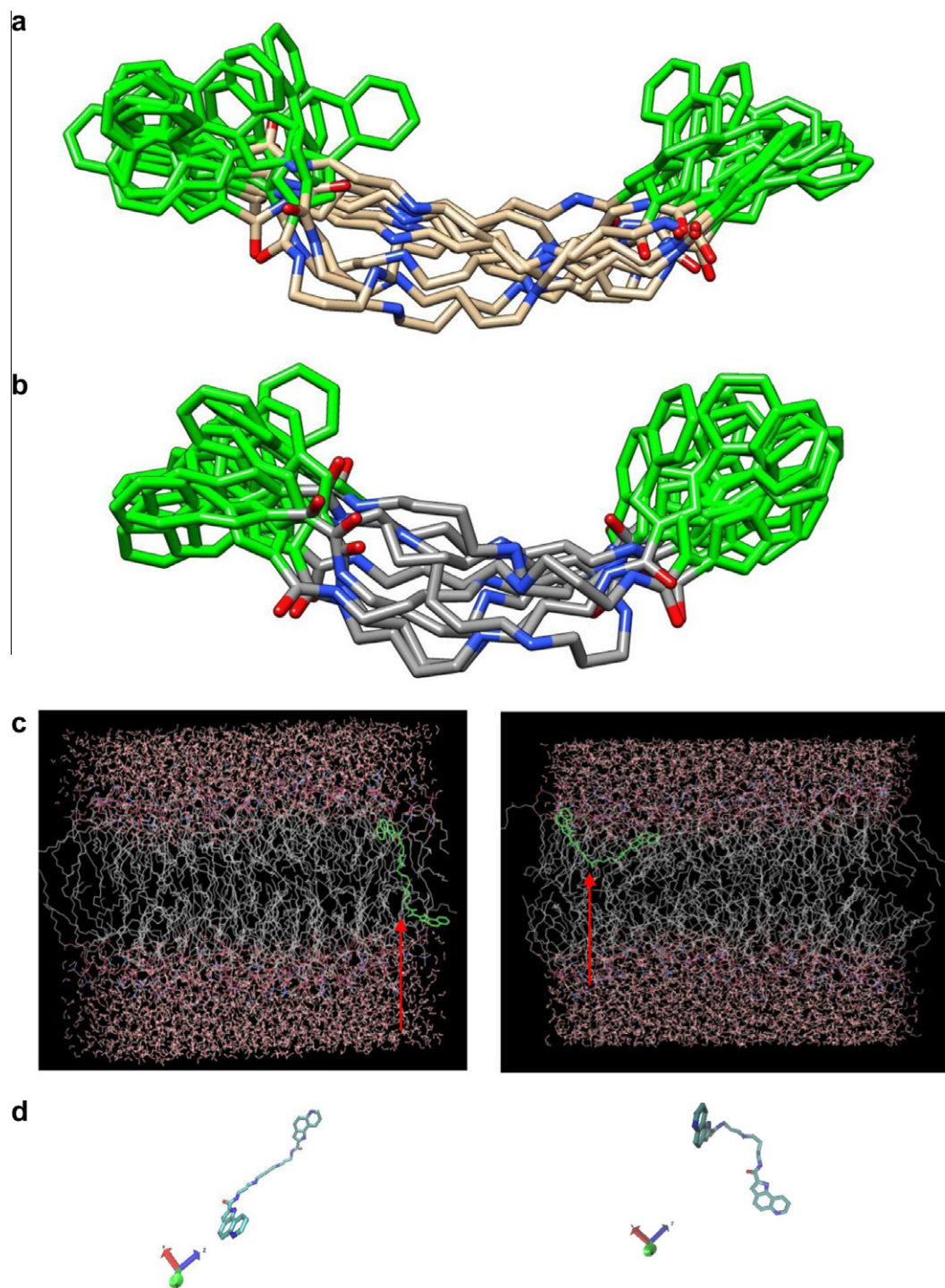


Figure 4. (top, left) **5e** in water, (top, right) **5e** in DMSO, (bottom, left) **5g** in water, (bottom, right) **5g** in DMSO.



**Figure 5.** Trajectory representations for compounds: (a) **5e** and (b) **5g**, into DMPC bilayer. Ten equally spaced snapshots throughout the last 20 ns of the simulation are shown. The aromatic rings are colored green and hydrogen atoms have been omitted for clarity. (c, left) **5e** in DMPC bilayer, (c, right) **5g** in DMPC bilayer. (d, left) Most preferable conformation of **5e** molecule in the DMPC bilayer, based on clustering calculations. (d, right) Most preferable conformation of **5g** molecule in the DMPC bilayer, based on clustering calculations.

Coulomb and Lennard-Jones interactions were calculated using a 1.0 nm cut-off.

Additional docking experiments with a different sequence, 1dne,<sup>25</sup> were also performed to cross-check the docking mode of the two compounds in DNA sequences (data shown in supporting information). Identical parameters were used for these calculations.

Docking experiments were designed according to previously published studies.<sup>26–29</sup>

### 3. Results and discussion

#### 3.1. Structure assignments of **5e** and **5g**

The <sup>1</sup>H NMR spectra of **5e** and **5g** were fully assigned by the use of a combination of 1D NMR and 2D homonuclear NMR spectroscopy. Proton resonances for both molecules were identified from integral inspection and chemical shifts of the <sup>1</sup>H NMR spectra, from the 2D DQF-COSY spectra and from the observed through-space

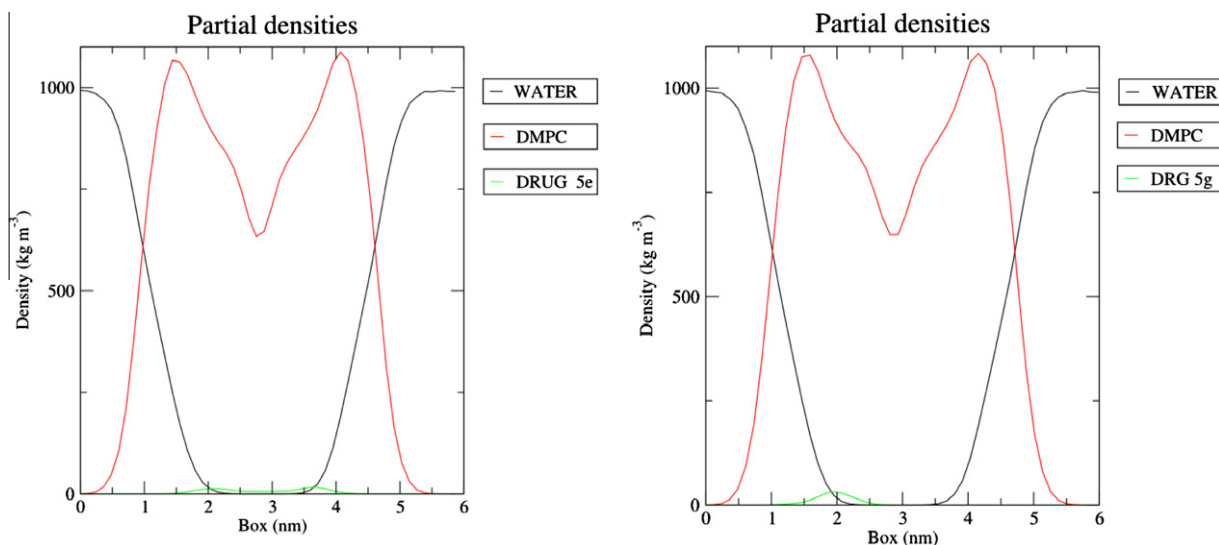


Figure 6. Mass density profile of **5e** embedded in lipid bilayer (left) and **5g** embedded in lipid bilayer (right).

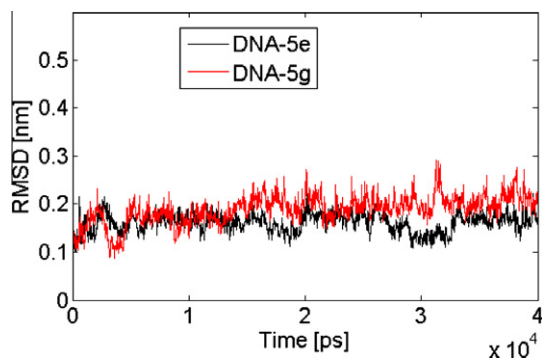


Figure 7. All-atom RMSD of DNA-bound molecules **5e** and **5g**, starting from the minimized structures and overlapped on the same structures.

proton correlations in the 2D NOESY spectra. The  $^1\text{H}$  NMR spectra of both **5e** and **5g** consist of two regions, one that accounts for the protons of the aromatic system and another for the protons of the aliphatic chain. Since **5e** and **5g** have similar structures, the assignment of protons in **5g** led directly to an assignment of **5e**. As it can be observed from Tables 1 and 2, both molecules present almost identical chemical shifts in the aromatic region. Figures 2 and 3 depict representative  $^1\text{H}$  NMR regions of the spectra of **5g** and **5e**, respectively. The strategy applied for the assignment of **5g** protons is briefly explained. H1/H1' that resonate at high field (13 ppm) and appear as singlet showed NOEs with H9/H9' (resonated at 9.15 ppm). The assignment of H9/H9' led through 2D DQF-COSY correlations to H8/H8' and subsequently to H7/H7'. 2D DQF-COSY experiment depicted the correlations between H1/H1'–H3/H3' (assigned at 7.30 ppm), H3/H3'–H4/H4' (assigned at 7.58 ppm) and H4/H4'–H5/H5' (assigned at 7.91 ppm). The protons of the amide bonds H10/H19 (resonated at 8.64 ppm) showed cross-peak signals in 2D DQF-COSY and NOESY experiments with H11/H18 (3.36–3.39 ppm). Subsequently, the 2D DQF-COSY experiment showed through bond correlation with H12/H13/H17 (assigned at 1.78 ppm, appears as a peak with quintet multiplicity and is integrated to 6H). Finally, H12/H13/H17 showed a DQF-COSY correlation with H14/H16 (assigned at 2.52–2.58 ppm). For the assignment of the structurally similar compound **5e**, the same strategy was applied.

After the full assignment of the  $^1\text{H}$  NMR spectra of **5e** and **5g**, the identification of critical NOEs for the two compounds was examined using 2D NOESY spectra. Critical NOEs lead to the determination of the orientation of the aliphatic chains of the molecules in relation to the aromatic segments. From the absence of long NOEs, using different mixing times and 2D ROESY experiments, it was concluded that both molecules receive extensive conformations in DMSO- $d_6$ .

### 3.2. Molecular dynamics simulations

MD simulations of **5e** and **5g** were initially performed in vacuum (supporting information), then in solvents (water and DMSO) and finally into DMPC lipid bilayer and in DNA complexes.

#### 3.2.1. MD simulations of **5e** and **5g** in water and DMSO

MD simulations were performed for the two molecules in water and DMSO using explicit solvent treatments. Each system was simulated for 40 ns. In both solvents, **5e** adopted primarily extended conformations, whereas **5g** showed a closed conformation in water with aromatic rings  $\pi$ – $\pi$  stacking (Fig. 4). Interestingly, this conformation (being present for 55% of the simulation time) predominated in vacuum (70%). In DMSO, both molecules adopted an extended conformation in accordance with the NMR data. These results suggest that **5e** stabilizes in an extended conformation in various media with different dielectric constants ( $\epsilon = 1$  for vacuum,  $\epsilon = 45$  for DMSO and  $\epsilon = 81$  for water), while **5g** adopts both extended and predominant closed conformations in water and in vacuum.

#### 3.2.2. MD simulations of **5e** and **5g** in DMPC bilayers

Drugs usually exert their biological activity after passing the aqueous barrier of membrane bilayers.<sup>30</sup> Since these molecules show cytotoxic activity, it would be of interest to examine their ability to penetrate into lipid bilayers. The two molecules were initially positioned in extended conformations at the aqueous layer of DMPC to examine if they pass the aqueous barrier and are incorporated spontaneously in the bilayer core. Trajectory representations of the two molecules are shown in Figure 5a and b. The most preferable conformations of the two molecules into DMPC, after eventually crossing the lipid bilayer, are shown in Figure 5c and d and are based on a clustering algorithm that is available in Chimera.<sup>31</sup> It was observed that **5e** spans the whole hydrophobic bilayer in an

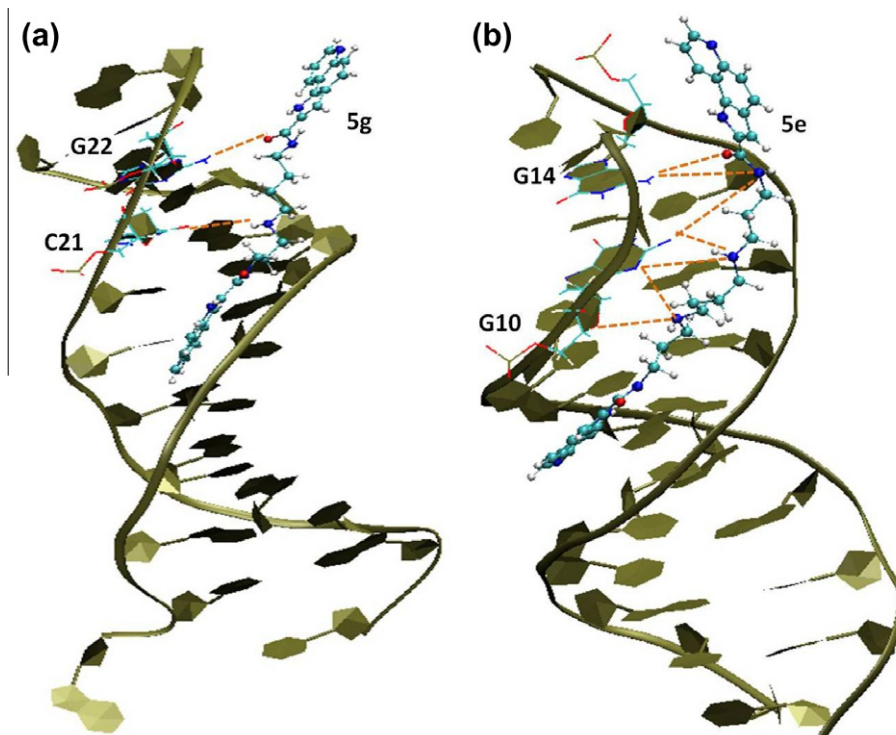


**Figure 8.** Docking of (a) **5g** and (b) **5e** in the crystal DNA sequence 1d64. Principal hydrogen bonding interactions are shown in dotted lines.

extended form, while **5g** spans one layer of the bilayer in a ‘semi-closed’ conformation (V-form). This shows that **5e** can be more easily accommodated into the lipid core, with the alkyl chain parallel to the corresponding alkyl chains of the lipid bilayers. This is, however, not the case for **5g**, where its alkyl chain is tilted with respect to the alkyl chains of DMPC. Thus, while **5g** appears to anchor onto the interface rather than the bilayer core, **5e** spans across the hydrophobic core. Consequently, this may indicate that **5g** will have more difficulty in penetrating the lipid bilayers than **5e**.

Figure 6 depicts their mass distribution along the Z-axis. These conformations can be clearly seen in the mass density profiles of **5e** and **5g** in lipid bilayers (Fig. 6).

The density profile of DMPC molecules along Z-axis is denoted with red color in Fig. 6 and shows higher mass in the head-group region because it contains the heavier atoms of oxygen, phosphorus and nitrogen, while the hydrophobic region that contains only carbon atoms and hydrogen atoms has lower mass. Compound **5e** (shown in green) spans over the hydrophobic region of the lipid bilayers. The maxima close to the interface of the lipid bilayers (green curve) probably represent the localization of the aromatic rings as they represent the most dense area of the compound. In the case of **5g**, there is a single maximum in the corresponding density profile due to its strong anchoring to the one leaflet, adopting a tilted conformation (see also Fig. 5).

A plausible explanation is that ring rigidity does not favor interactions with the flexible alkyl chains. Generally, rigid rings tend to localize in the upper segment of alkyl chains and close to the interface rather than deeply into the alkyl chain region (e.g., the tricyclic segment of cholesterol prefers the upper part of the alkyl chain and interface and its alkyl chain is embedded into the center of the bilayer). Such an orientation may hinder the movement towards the interior of the cell. Interestingly, in **5e** due to the reduced flexibility of alkyl chain (interrupted by the two –NH groups), the aromatic rings scavenge both the interface and deeply towards the center of the bilayer.

Compound **5g** does not show any density around the center of the bilayer, indicating that its interaction is limited in the interface region and upper hydrophobic segment of the lipid bilayers. Nonetheless, both molecules are incorporated in the bilayer core and spontaneously anchor adopting a different orientation and localization. Another important structural property is the area per lipid, which is defined as the product of X and Y dimensions divided by the number of lipid molecules in each leaflet (64 in this case). The area per lipid is a diagnostic tool of the mesomorphic state of the lipid bilayer. For the systems with **5g** and **5e** molecules, the above-mentioned quantity is equal to  $0.635 \pm 0.003$  and  $0.632 \pm 0.005$  nm<sup>2</sup>/lipid, respectively. Indeed, this value corresponds to a lipid bilayer that is found in the liquid-crystalline phase as expected by the temperature of the simulations (310 K).

### 3.2.3. Docking and molecular dynamics of **5e** and **5g** bound to DNA

An early convergence of the simulations denoted the structural stability of both DNA-bound systems (Fig. 7). Hydrogen bonding analysis was done through appropriate GROMACS tools,<sup>8</sup> which use standard geometrical criteria such as distance between acceptor and donor (<0.35 nm) and the angle among acceptor–hydrogen–donor (<30°). Compound **5e** cross-links with the 1d64 DNA sequence, resulting in several hydrogen bonding interactions between nitrogen and oxygen atoms of the drug and DNA bases guanine 10/14 (Fig. 8). Compound **5g** displayed a less extensive hydrogen bonding network with 1d64, as it only formed two hydrogen bonds with guanine22 and cytosine21. This may partially rationalize the increased binding affinity of **5e** toward DNA. MD simulations of the complex DNA-**5e** in water further confirmed its stability, with **5e** adopting an extended conformation. In particular, the angle among atoms 2-16-2' (Fig. 1) is monitored during the course of the simulation to be  $146^\circ \pm 3^\circ$ . Compound **5g** also adopted an extended conformation as seen by the angle 2-15-2', which was found to be  $167^\circ \pm 1^\circ$ .

**Table 3**  
Docking scores and binding free energies of **5e** and **5g** with 1d64 DNA sequence

Compound	Docking score (glide) in kcal/mol	Binding energy (LIE method) in kcal/mol
<b>5e</b>	−13.094	−14.96 (3.70)
<b>5g</b>	−9.695	−12.74 (3.33)

Similar results were obtained for **5e** with the crystal DNA sequence 1dne (data not shown). Compound **5e** cross-links with 1dne DNA sequence, resulting in enhanced hydrogen bonding, similar to 1d64.

In addition to the previously described computations, the binding free energy was estimated through the Linear Interaction Energy (LIE) method,<sup>32</sup> in which two different MD simulations are needed: one of the total system with the drug bound to the DNA at the position indicated by the docking calculations and one of the drug placed in pure solvent (water). An estimate for the binding free energy is given by the following equation:

$$\Delta G_{\text{bind}} = a\Delta V^{\text{vdw}} + \beta\Delta V^{\text{el}} \quad (1)$$

where the differences  $\Delta V^{\text{vdw}}$ ,  $\Delta V^{\text{el}}$  are the MD averages of the non-bonded (van der Waals) and electrostatic interactions of the ligand in the free (pure solvent) and bound states. The adjustable parameters  $a$ ,  $\beta$  of Eq. 1 were assigned to 0.181 and 0.500, respectively, and a full description of the method and how it is applied in GROMACS can be found elsewhere.<sup>8,32</sup> The values of parameters in Eq. 1 are the same for both systems due to the similarity of the molecules (**5e** and **5g**) that are bound at the same position of the DNA helix. The binding free energies are summarized in Table 3 and they are compared to the estimates obtained by the docking computations. An interesting observation was that **5e** binds more efficiently than **5g** and consequently it is more suitable as a cross-linking probe due to its ability to interact more strongly with the two helices of the DNA. It is important to note that although the LIE method is considered as more accurate than docking calculations, its usefulness is primarily focused on the estimation of the difference between the binding energies of two complexes rather than the accurate prediction of their absolute binding energies.

Furthermore, it was observed that **5e** cross-links with both nucleotide sequences, whereas **5g** cross-links with only the 1dne nucleotide sequence. Irrespective of the initial conformation of the ligand, docking calculations showed that it always acquired extended conformations.

#### 4. Conclusions

Cytotoxic molecules are well known to interact with DNA nucleotide sequences and to interfere with their replication. However, in order to reach their site of action in the nucleus of the cell, these molecules must first cross the lipid bilayer barrier. To understand the mechanism of action of two novel cytotoxic C2-substituted pyrolo[2,3-*f*]quinolines, we have explored their conformations in different media and their ability to be incorporated into the lipid bilayers. Although the two molecules have similar chemical structures, they adopted different conformations. In silico calculations revealed that **5e** adopted primarily an extended conformation in media varying in dielectric constants, in agreement with NOE data. Compound **5g** was additionally found to acquire semi-closed (V-shaped) or even closed conformations in water and in vacuum. The most striking difference between the two molecules was observed after they were initiated for MD calculations in the aqueous layer and spontaneously permeated into the DMPC lipid core: **5e** was incorporated into the lipid core in an extended conformation

and in a fashion that its alkyl segment was parallel to the alkyl chains of the lipid bilayers. Such an orientation facilitates its passage to the cytoplasm and finally to the nucleus. On the other hand, **5g** anchors at the interface in an unusual way. Its alkyl chain is tilted with respect to the alkyl chains of the phospholipids. Aromatic rings in **5g** are localized in the interface region. Such an orientation of aromatic rings has been suggested by several previous studies.<sup>33–36</sup>

Regarding their interactions with DNA nucleotide sequence, **5e** binds more favorably than **5g**, forming an enhanced hydrogen bonding network and cross-links. Such strong interactions by **5e** establish that not only does it reach more easily its target but it also induces stronger binding effects. In conclusion, the combination of experimental and theoretical methodologies applied may provide a plausible explanation of the efficient cytotoxic effects of **5e**.

#### Acknowledgments

This work was partially supported by funding provided by the European Commission for the FP7-REGPOT-2009-1 Project 'ARCADE' (Grant Agreement No. 245866).

#### References and notes

- Miliard, J. T.; Weidner, M. F.; Kirchner, J. J.; Ribeiro, S.; Hopkins, P. B. *Nucleic Acids Res.* **1991**, *19*, 1885.
- Subhas Bose, D.; Thompson, A. S.; Ching, J.; Hartley, J. A.; Berardini, M. D.; Jenkins, T. C.; Neidle, S.; Hurley, L. H.; Thurston, D. E. *J. Am. Chem. Soc.* **1992**, *114*, 4939.
- Tsotinis, A.; Vlachou, M.; Zouroudis, S.; Jeney, A.; Timer, F.; Thurston, D. E.; Roussakis, C. *Lett. Drug Des. Discovery* **2005**, *2*, 189.
- Tsotinis, A.; Vlachou, M.; Gerasimopoulou, M.; Eikosipentaki, A.; Ioannidis, C.; Ktovidaki, A.; Afroudakis, P. A.; Moreau, D.; Roussakis, C. *Lett. Drug Des. Discovery* **2007**, *4*, 87–91.
- Schuttelkopf, A. W.; van Aalten, D. M. F. *Acta Crystallogr.* **2004**, *60*, 1355.
- Berendsen, H. J. C.; van der Spoel, D.; van Drunen, R. *Comp. Phys. Commun.* **1995**, *91*, 43.
- Van der Spoel, D.; Lindahl, E.; Hess, B.; Groenhof, G.; Mark, A. E.; Berendsen, H. J. C. *J. Comp. Chem.* **2005**, *26*, 1701.
- Van der Spoel, D.; Lindahl, E.; Hess, B.; van Buuren, A. R.; Apol, E.; Meulenhoff, P. J.; Sijbers, A.; Feenstra, K. A.; van Drunen, R.; Berendsen, H. J. C. *GROMACS User Manual*, version 4.5; Nijenborgh 4, 2010. [www.gromacs.org](http://www.gromacs.org).
- Wang, J.; Wolf, R. M.; Caldwell, J. W.; Kollman, P. A.; Case, D. A. *J. Comput. Chem.* **2004**, *25*, 1157.
- Jakalian, A.; Bush, B. L.; Jack, D. B.; Bayly, C. I. *J. Comput. Chem.* **2000**, *21*, 132.
- Jakalian, A.; Jack, D. B.; Bayly, C. I. *J. Comput. Chem.* **2002**, *23*, 1623.
- Berendsen, H. J. C.; Postma, J. P. M.; DiNola, A.; Haak, J. R. *J. Chem. Phys.* **1984**, *81*, 3684.
- Essmann, U.; Perera, L.; Berkowitz, M. L.; Darden, T.; Lee, H.; Pedersen, L. G. *J. Chem. Phys.* **1995**, *103*, 8577.
- Berendsen, H. J. C.; Postma, J. P. M.; van Gunsteren, W. F.; Hermans, J. In *Intermolecular Forces*; Pullman, B., Ed.; D. Reidel: Dordrecht, 1981; pp 331–342.
- Tielemann, D. P.; Berendsen, H. J. C. *J. Chem. Phys.* **1996**, *105*, 4871.
- Berger, O.; Edholm, O.; Jahnig, F. *Biophys. J.* **2002**, *1997*, 72.
- Hess, B.; Bekker, H.; Berendsen, H. J. C.; Fraaije, J. *J. Comput. Chem.* **1997**, *18*, 1463.
- Sybyl Molecular Modeling Software. Tripos International, 1699 South Hanley Rd., St. Louis, Missouri 63144, U.S.A.
- Van Gunsteren, W. F.; Berendsen, H. J. C. *J. Mol. Biol.* **1984**, *176*, 559.
- Van Gunsteren, W. F.; Berendsen, H. J. C. *Angew. Chem., Int. Ed. Engl.* **1990**, *29*, 992.
- Edwards, K. J.; Jenkins, T. C.; Neidle, S. *Biochemistry* **1992**, *31*, 7104.
- Glide, Version 5.0, User Manual, Schrödinger, LLC, New York, NY, 2008.
- Schrödinger Suite 2009 Protein Preparation Wizard; Epik Version 2.0, Schrödinger, LLC, New York, NY, 2009.
- Duan, Y.; Wu, C.; Chowdhury, S.; Lee, M. C.; Xiong, G.; Zhang, W.; Yang, R.; Cieplak, P.; Luo, R.; Lee, T.; Caldwell, J.; Wang, J.; Kollman, P. *Comput. Chem.* **1999**, *2003*, 16.
- Coll, M.; Aymami, J.; Van der Marel, G. A.; Van Boom, J. H.; Rich, A. *Biochemistry* **1989**, *28*, 310.
- Vargiu, A. V.; Ruggerone, P.; Magistrato, A.; Carloni, P. *Biophys. J.* **2008**, *94*, 550.
- Suckling, C. J. *J. Phys. Org. Chem.* **2008**, *21*, 575.
- Numm, C. M.; Garman, E.; Neidle, S. *Biochemistry* **1997**, *36*, 4792.
- Janovec, L.; Kozurkova, M.; Sabolova, D.; Ungvarsky, J.; Paulikova, H.; Plsikova, J.; Vantova, Z.; Imrich, J. *Bioorg. Med. Chem.* **2011**, *19*, 1790.
- Lucio, M.; Lima, J. L. F. C.; Reis, S. *Curr. Med. Chem.* **2010**, *17*, 1795.
- Petterson, E. F.; Goddard, T. D.; Huang, C. C.; Couch, G. S.; Greenblatt, D. M.; Meng, E. C.; Ferrin, T. E. *J. Comput. Chem.* **2004**, *25*, 1605.
- Aqvist, J.; Luzhkov, V. B.; Brandsdal, B. O. *Acc. Chem. Res.* **2002**, *35*, 358.

33. Maier, T. J.; Schiffmann, S.; Wobst, I.; Birod, K.; Angioni, C.; Hoffmann, M.; Lopez, J. J.; Glaubitz, C.; Steinhilber, D.; Geisslinger, G.; Grosch, S. *J. Mol. Med.* **2009**, *87*, 981.
34. Potamitis, C.; Chatzigeorgiou, P.; Siapi, E.; Mavromoustakos, T.; Hodzic, A.; Cacho-Nerin, F.; Laggner, P.; Rappolt, M. *Biochim. Biophys. Acta* **2011**, *1808*, 1753.
35. Ntountaniotis, D.; Malis, G.; Grdadolnik, S. G.; Halabalaki, M.; Skaltsounis, A.-L.; Potamitis, C.; Siapi, E.; Chatzigeorgiou, P.; Rappolt, M.; Mavromoustakos, T. *Biochim. Biophys. Acta* **2011**, *1808*, 2995.
36. Hodzic, A.; Zoumpoulakis, P.; Pabst, G.; Laggner, P.; Mavromoustakos, T.; Rappolt, M. *Phys. Chem. Chem. Phys.* **2012**, *14*, 4780.